ELSEVIER

PII: S0032-3861(98)00019-6

Polymer Vol. 39 No. 20, pp. 4773–4783, 1998

0032-3861/98/$19.00+0.00

Mechanical properties of plasticized poly(vinylchloride): effect of drawing and filler orientation

Isabelle Fras[a], Micheline Boudeulle[b], Philippe Cassagnau[a] and Alain Michel[a,*]
[a]*C.N.R.S., Laboratoire des Matériaux Organiques à Propriétés Spécifiques, B.P. 24, 69390 Vernaison, France*
[b]*Université Claude Bernard Lyon I, Laboratoire de Physico-Chimie des Matériaux Luminescents, UMR5620, Bât.205-43, Bd du 11 Novembre 1918, 69622, Villeurbanne, Cédex, France*
(Received 22 July 1997; revised 5 November 1997; accepted 1 December 1997)

Reinforcement of plasticized poly(vinylchloride) was achieved by the use of two anisotropic fillers: talc and a lead carboxylate. The orientation of such fillers was developed during the extrusion processing. Then, in the present paper, we studied the correlations between extrusion conditions (draw ratio, temperature), development of particle orientation (talc, lead stabilizer) and tensile properties of a plasticized polyvinylchloride. X-ray diffraction measurements have allowed us to analyse orientation of the particles which also became evident through tensile property results. This work shows that talc is a good candidate for filling PVC formulations. Furthermore, good orientation is achieved with the extrusion conditions used. Moreover, the orientation of the lead stabilizer which has a lamellar shape leads to an increase in Young's modulus. The enhancement of the Young's modulus obtained by these two fillers is well modelled by the Halpin and Tsai law, considering that the platelets are oriented in the stretching direction. Concerning drawing, the stretching temperature has proved to be of particular importance, especially when it is above or below the temperature of the 'gel–liquid' transition of PVC, found to be around 205°C.

(Keywords: plasticized poly(vinylchloride); drawing; filler orientation)

INTRODUCTION

Fillers have increasingly gained importance in the thermoplastic industry. Reinforcement of filled polymers is generally achieved by the use of highly anisotropic fillers, e.g. fibres and flake-like minerals (talc, kaolin, mica, etc.)[1,2]. The orientation of such fillers may be developed during processing operations as proposed in Jeffery's theory, and predicted by Vincent and Agassant [3] in the case of injection molding. Processing conditions themselves can influence the degree of orientation. Quantitative data on the orientation of talc and mica have been determined by Monge et al. [4] in injection-molded 6,6-polyamide, and by Lim and White [5] in a low density polyethylene under different processing operations. Flake-like fillers tend to be parallel to the surface of the extruded or injection-molded material, with a more pronounced effect in the skin than in the core. Crowson et al. [6] have shown that glass fibres orientation is greatly enhanced by increasing shear rate or by decreasing die-length of a capillary rheometer.

Among the more popular techniques used to characterize filler orientation, X-ray diffraction presents many advantages. By the pole-figure analysis, it can give quantitative three-dimensional orientation distribution of different shaped particulates in the same experiment [7]; it can differentiate the orientation of a crystalline polymer and that of the particle fillers. Glass fibre orientation has been determined by Darlington and McGinley [8] (X-ray radiography of 100-mm-thick slices).

In practice, on the other hand, polymeric materials, e.g. electrical wire coatings, are usually used in the form of oriented polymers. Two interesting studies revealed the importance of the spherical filler diameter [9] on the reinforcement of a rigid PVC, and that of the adhesion between the filler and the matrix preventing the voids formation during drawing [10].

Thus, the purpose of this paper is to study the correlations between the extrusion conditions (draw ratio, temperature), the orientation of a mineral filler, talc, and a lead carboxylate (PVC heat stabilizer) in the solid form at the extrusion temperature, and tensile properties of a plasticized polyvinylchloride. X-ray diffraction measurements were used to analyse the platelet orientation. The model developed by Halpin and Tsai which has proved to predict correctly the tensile behaviour of polymers filled with flake-like fillers fully oriented has been used in this work.

EXPERIMENTAL

Material

A suspension PVC (Evipol SH 8020), supplied by the European Vinyl Corporation, is used. The plasticizer (Bisoflex T810T) is a nonyl trimellitate and is supplied by B.P. Chemicals. The mineral filler is a talc (00S), commercialized by Talc de Luzenac. Two kinds of heat stabilizers were used: a tin thioglycolate stabilizer (Stavinor T890) from Ceca for formulations filled with talc only and a lead carboxylate (8831/E) from La Floridienne Chimie. This lead stabilizer can be described as flakes with an ellipsoidal shape, and is considered in this study either as a filler used

* To whom correspondence should be addressed

Table 1 Formulations and notations, ϕ_v: volume fractions

	Heat stabilizer Tin stabilizer	Lead stabilizer
Formulation (weight parts of additives for 100 parts of PVC):		
PVC	100	100
Plasticizer	50	50
Stabilizer	2	$3 \leq x \leq 12 \rightarrow 0.0075 \leq \phi_v \leq 0.02$
Talc	$0 \leq y \leq 13$	$3 \leq y \leq 13 \rightarrow 0.011 \leq \phi_v \leq 0.0156$
Notation	PVC_{Sn2Tay}	PVC_{PbxTav}

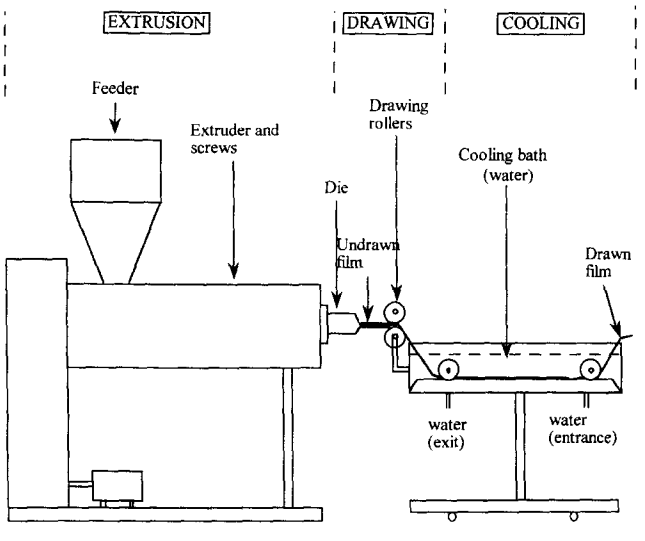

Figure 1 Scheme of the processing operation (extrusion followed by a drawing step)

alone in the formulations or with the other filler, talc, but never in the presence of the tin thioglycolate stabilizer.

Information concerning the formulations is given in *Table 1*. The physical characteristics of the two fillers (talc and lead stabilizer) are quoted in *Table 2*.

Sample preparation

The dry-blends were first extruded to cause gelation of PVC and then granulated. This first step was achieved on a Clextral BC 21 (*L/D* = 24) twin-screw (co-rotating) extruder at a screw speed of 550 rpm, an output of 25 kg/h and a temperature set at 170°C in the last zone. In a second step, these granules were extruded with a twin-screw (counter-rotating) Leistritz LSM 30-34 (*L/D* = 16.5) extruder to form a strip which is drawn before cooling, as illustrated in *Figure 1*.

Melt temperature and pressure were controlled with sensors assembled on the die, as schematically representated in *Figure 2*.

The melt temperature is controlled by the thermal sensor plunging into the polymer melt at half-height. Pressure control along the die permits evaluation of the

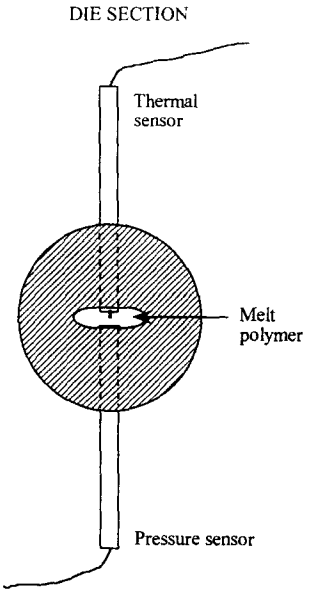

Figure 2 Slit die section: thermal and pressure sensors location

apparent wall stress and then the apparent viscosity of the polymer.

In this study, melt draw was performed at 190 and 210°C. These temperatures were reached by setting the temperature of the different zones of the extruder at 175 and 200°C, respectively. The screw speed was 100 rpm and the shear rate at the die was 30 s^{-1}, the flow rate was 10 kg/h.

Tensile properties

Standard H3 dumb-bells (from the French standard NF T 51034) were cut in the film parallel to the draw axis. The thickness of the samples varies from 0.5 to 2 mm (due to drawing during processing), but this variation has no significant influence on the tensile results. Ten test samples were used to evaluate the tensile properties. Tensile tests were carried out at room temperature using an Instron 1175 tensile tester at 50 mm min^{-1} grip separation speed. Young's modulus was calculated when determining the stress–strain curve tangent slope at low deformations and using the area of the initial cross-section. Elongation at break was calculated from the initial and final grip separations.

X-ray diffraction measurements

Powder method by diffractometry. Test samples were cut into square-shaped pieces of about 1 cm^2 area. X-ray diffractograms were obtained with a powder diffractometer Siemens D500 operating at 35 kV and 30 mA. CuKα radiation (λ = 1.540 Å) was filtered through a back graphite monochromator. Data were recorded according to a step-scan procedure with a step of 2°(2θ) and a counting time of 1 or 2 s.

Table 2 Talc and lead stabilizer characteristics

	Density (g/cm^3)	Aspect ratio (*L/D*)	d_{50} (μm)[a]	T_{fusion} (°C)	Tensile modulus (Pa)
Talc	2.78	7	2		1.2074×10^{11}
Lead stabilizer	5.43	60		130	-

[a] d_{50} is the average diameter when the cumulative weight percent of filler is equal to 50. This value of d_{50} is taken according to the particle distribution measurement.

Table 3 Theoretical models of Young's modulus for filled polymers

Model	Equation	
Einstein	$E_R = 1 + 2.5\phi$	(1)
Guth–Smallwood	$E_R = 1 + 2.5\phi + B\phi^2$	(2)
	B is usually 14.1	
Kerner	$E_R = \dfrac{G_p\phi/[(7-5\nu)G_m + (8-10\nu)G_p] + \phi/[15(1-\nu)]}{G_m\phi/[(7-5\nu)G_m + (8-10\nu)G_p] + \phi/[15(1-\nu)]}$	(3)
Nielsen	$E_R = \dfrac{1+A\phi}{1-\psi\phi}$	(4)
	$\psi = 1 + [(1-\phi_m)/\phi_m^2]\phi$	(5)
	$A = f$(geometry)	(6)

E_R is the relative modulus; ϕ the filler volume fraction; G_p the shear modulus of filler; G_m the shear modulus of the matrix; ν the Poisson ratio of polymer; ϕ_m the maximum packing fraction of filler.

Monochromatic pinhole technique. Flat thin samples (thickness smaller than 1 mm) were analysed by transmission and diffracted beams were recorded on a disc-like photographic film for 8–10 h. Ni-filtered CuKα radiation was used and passed through collimators separated from the sample by a distance of 2–3 mm. The photographic film was 50 mm away from the sample.

Transmission electron microscopy

Ultrathin sections for transmission electron microscopy (TEM) were prepared. TEM photographs were taken by a JEOL 1200 EX electron microscope at an accelerating voltage of 80 kV. Additional heavy metal staining was not required; sufficient contrast for TEM was obtained with unmodified specimens.

Mechanical predictive models of filled polymers

Modulus. The modulus of filled materials [1] has been representated by a large number of equations. Among the most prominent are those of Einstein, Guth–Smallwood, Kerner and Nielsen. These models, given for spherical particles, are listed in *Table 3*.

Einstein's equation is applicable only for materials filled with low concentrations of non-interactive spheres. Guth–Smallwood's equation takes into account interparticle interactions at higher filler concentrations. Nielsen's equation is a modification of the Kerner's model taking into account both the maximum packing fraction of the filler, interparticle interactions and the relative modulus of the two constituents.

In the case of flake-like fillers added to polymers, the relative modulus is often predicted by the Halpin and Tsai model. Halpin and Tsai [11] proposed a law, which can be approximated to an extension of the Voigt and Reuss models, to predict the longitudinal and transversal moduli of a composite filled with fully oriented fibres. In the case of flake-like fillers, transversal and longitudinal moduli are equivalent [equation (7)].

$$\frac{E_c}{E_m} = \frac{1+\xi\eta\phi_p}{1-\eta\phi_p} \tag{7}$$

with

$$\xi = 2(d/h) \text{ and } \eta = \frac{E_p - E_m}{E_p + \xi E_m} \tag{8}$$

where E_c is the composite modulus in the direction of the platelets orientation; E_m is the matrix modulus; d is the average diameter of the filler; h is the average thickness of the filler; ϕ_p is the volume fraction of the filler; E_p is the filler modulus.

Mitsuishi et al. [10] modified this equation in the case of a drawn polypropylene filled with talc (or mica) to enable this model to fit the experimental results. The modification is as follows:

$$\frac{E_c}{E_m} = \frac{1+\xi * \eta * \phi_p}{1-\eta * \phi_p}\frac{1-\phi_v}{1+\phi_v/\delta} \tag{9}$$

with

$$\xi * = 2\beta d/h \text{ and } \eta * = \frac{\gamma E_p - E_m}{\gamma E_p + \xi * E_m} \tag{10}$$

where β and γ are adjustable parameters; ϕ_v is the void volume fraction in the oriented polymer matrix; and δ is the void length to void thickness ratio.

Elongation at break. A modified Nielsen's [1] law is often used to predict the composite's elongation at break (in the case of spherical particles with good adhesion to matrix):

$$\epsilon_c/\epsilon_m = (1 - K\phi^{2/3}) \tag{11}$$

where ϕ is the volume fraction of filler and K is an adjustable parameter taking into account the filler geometry.

RESULTS AND DISCUSSION

Mineral particles

X-ray diffraction. When the melt processing temperature is 210°C, evidence of talc orientation in a sample filled with 13 phr of talc and drawn with $\lambda = 5$ ($PVC_{Sn2Ta13/\lambda=5}$) can be deduced from *Figure 3*.

Compared to talc with a random distribution orientation (*Table 4*), only reflections from the (00l) planes appear. That clearly means that these talc cleavage planes are parallel to the surface of the analysed sample (i.e. to the extrudate surface). We attribute the small peaks at $d = 7.107$, 3.553, 2.892 Å to chlorite, present in talc at low concentrations, meaning that these layered silicate particles are oriented together with talc.

Furthermore, *Figure 3* compares talc orientation in the core and in the skin of the extrudate: no other crystallographic plane diffracts in the core nor can higher diffraction intensities be detected in the skin. So, no core–skin orientation distribution was detectable, as is the case in injection-molded samples [9]. Our results are consistent with those of Lim and White [5], who noticed by pole figure

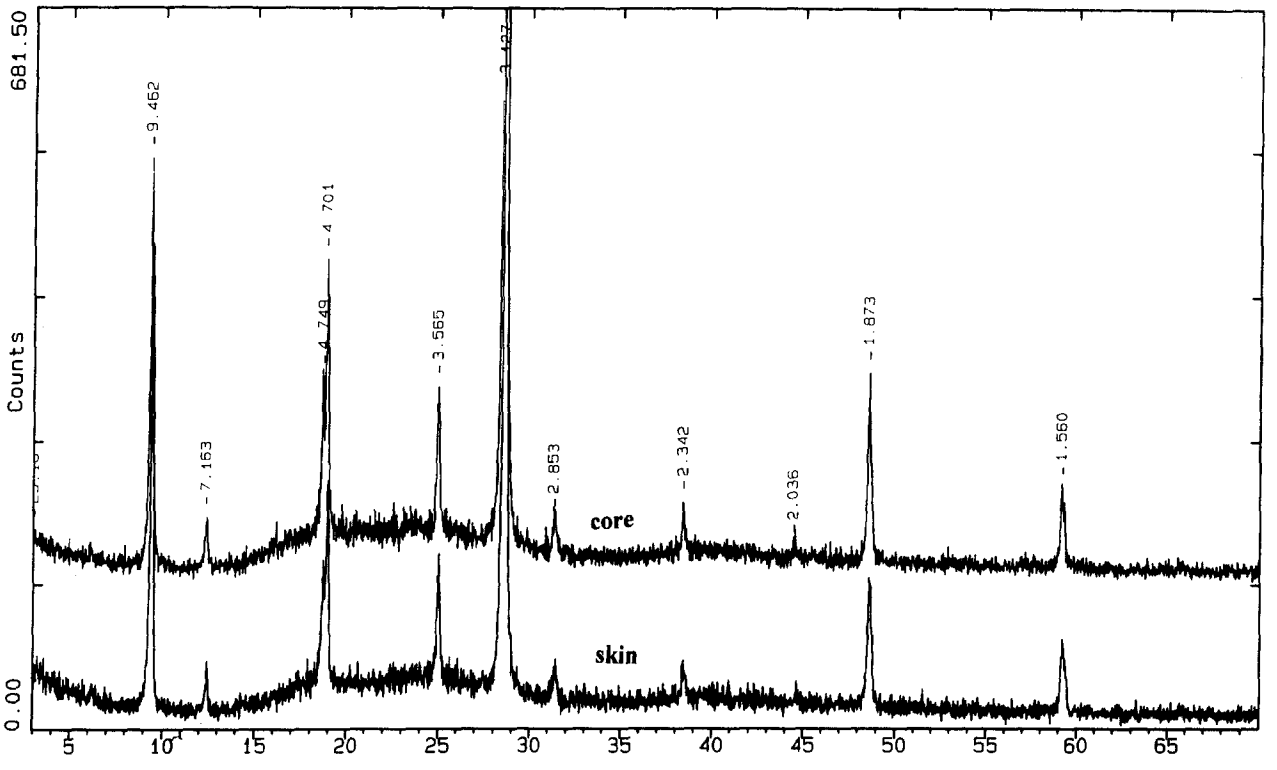

Figure 3 X-ray diffractometer scans of a 13 phr talc-filled sample extruded at 210°C and drawn with $\lambda = 5$, $PVC_{Sn2Ta13/210°C/\lambda=5}$: core–skin orientation distribution

Table 4 X-ray diffractometer data of a standard talc, free of magnesite (file no. 13-558 of JCPDS-ICDD)

d (Å)	Intensity	h k l
9.34	100[a]	0 0 2
4.66	90[a]	0 0 4
4.55	30	−1 1 1
3.51	4	−1 1 4
3.43	1	1 1 3
3.116	100[a]	0 0 6
2.892	1	0 2 5
2.629	12	−2 0 2
2.595	30	−1 3 2
2.476	65	1 3 2
2.335	16[a]	0 0 8
2.212	20	2 2 1
2.196	10	−2 0 6
2.122	8	2 0 4
2.103	20	−1 3 6
1.930	6	2 2 4
1.870	40[a]	0 0 10
1.725	2	−2 4 2
1.682	20	1 5 2
1.557	20[a]	0 0 12
1.527	40	0 6 0
1.509	10	3 3 0
1.460	8	3 3 2
1.406	16	3 1 6
1.394	20	−1 3 12

[a]Enhanced by orientation.

analysis that talc was nearly fully oriented during capillary die or sheet extrusion (Hermans particle orientation factor f_H was about −0.5) for an apparent shear rate between 2 and 1000 s^{-1}. This orientation is draw-ratio independent, since no difference was noticeable between these diffractometer scans and those made in the case of the same formulation drawn with a higher draw ratio.

Talc orientation in the extrudate plane has also been confirmed by electron diffraction patterns from thin cuts of the talc-filled PVC sample observed by transmission electron microscopy (*Figure 4*).

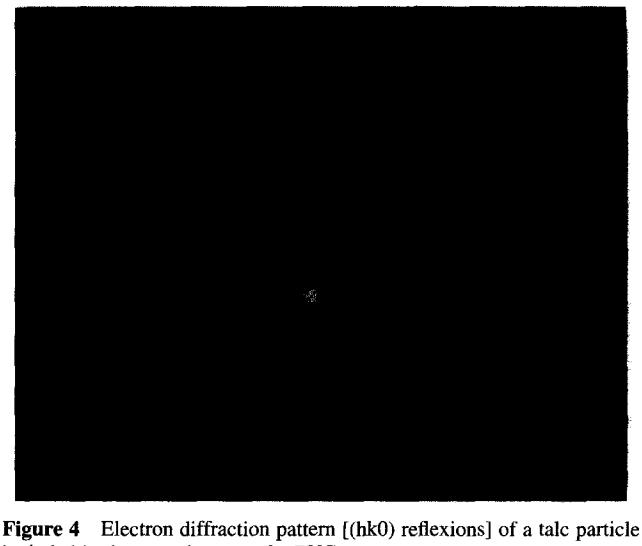

Figure 4 Electron diffraction pattern [(hk0) reflexions] of a talc particle included in the extrudate sample, $PVC_{Sn2Ta13}$

This pattern presents hk0 reflections [(001)* planes in the reciprocal lattice], which means that the incident electron beam is parallel to the axes [001], almost perpendicular to the talc platelets (monoclinic lattice).

Concerning the temperature influence on talc orientation, we can deduce from these experiments that it does not play any role in the orientation, since no difference was observed between X-ray scans recorded on talc-filled samples drawn at 190 or 210°C.

Linear viscoelastic characterization. Dynamic mechanical measurements were made using a Rheometrics

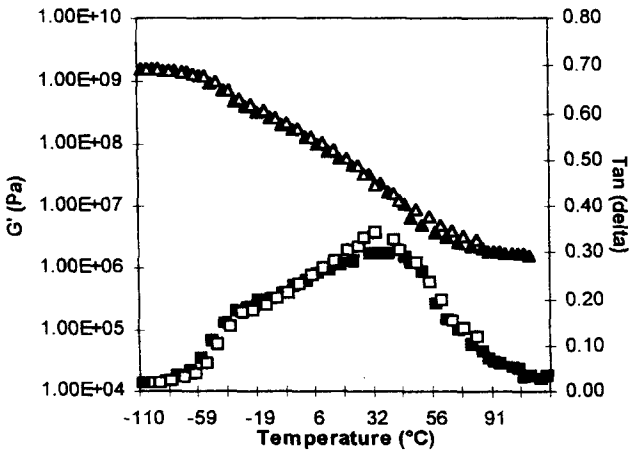

Figure 5 Variation of elastic modulus and loss angle tangent in the glass transition region in the presence or not of talc. Elastic modulus is represented by: (▲) PVC_{Sn2}; (△) $PVC_{Sn2Ta13}$ and the loss angle tangent is represented by: (■) PVC_{Sn2}; (□) $PVC_{Sn2Ta13}$

RMS 800 spectrometer. Dynamic moduli were measured with two sample shapes, depending on temperature:

(1) When the temperature is lower than 130°C, a strip sample (10 mm wide, 45 mm long and 1 mm thick) is used. The sample is mounted between specially designed film grips with the long axe positioned in the vertical direction.
(2) When the temperature is higher than 130°C, a disc-like shaped sample (diameter: 7.9 mm, thickness: 1 mm) is used and placed between two rough plates.

The first point of interest is the comparison between the dynamic mechanical response of unfilled (PVC_{Sn2}) and filled ($PVC_{Sn2Ta13}$) formulations. This was achieved through measurements in the glass transition region, by a temperature sweep. Frequency was fixed at 0.3 rad/s and the strain was increased from 0.05 to 1%. Results are reported in *Figure 5*, which lead to the conclusion that talc does not modify the dynamic moduli of the PVC nor its glass transition. Two relaxations are distinguished: the α relaxation (at 35°C), associated to the glass transition of the system and the second order, or β relaxation, (at −40°C). This β relaxation has already been reported to occur around this temperature [12] and the α relaxation of this system is higher than that obtained in the case of a 50 phr diisooctyle phthalate-plasticized PVC [13], where it is found to be −30°C. This observation is mainly due to the difference in molecular weight of these two plasticizers.

The second point of interest is the dynamic mechanical response of PVC when the temperature becomes close to that of the extrusion process. *Figure 6* shows the dynamic mechanical behaviour of the reference formulation (PVC_{Sn2}) according to temperature (frequency: 0.3 rad/s).

The curves of the elastic and viscous modulus cross in the region of 200–210°C. The change of the loss angle tangent with frequency and temperature is reported in *Figure 7*. At 205°C, the loss angle tangent is frequency independent. So, this temperature can be assumed to be the 'gel–liquid' transition temperature of the PVC. This temperature is very close to that already found by others [13,14] in the case of plasticized polyvinylchloride and is not modified in the presence of talc. So, from these rheological properties, we can deduce that talc filler does not modify the linear dynamic mechanical behaviour of the polymer in the volume fraction range studied here.

So, we chose two extrusion temperatures: higher than 205°C where the plasticized PVC tends to be in a viscoelastic liquid state and lower than 205°C, where the PVC is in a viscoelastic gel state.

Tensile properties

Processing melt temperature $T = 210$°C

The effect of draw ratio on relative Young's modulus of unfilled plasticized PVC (PVC_{Sn2}) is shown in *Figure 8*.

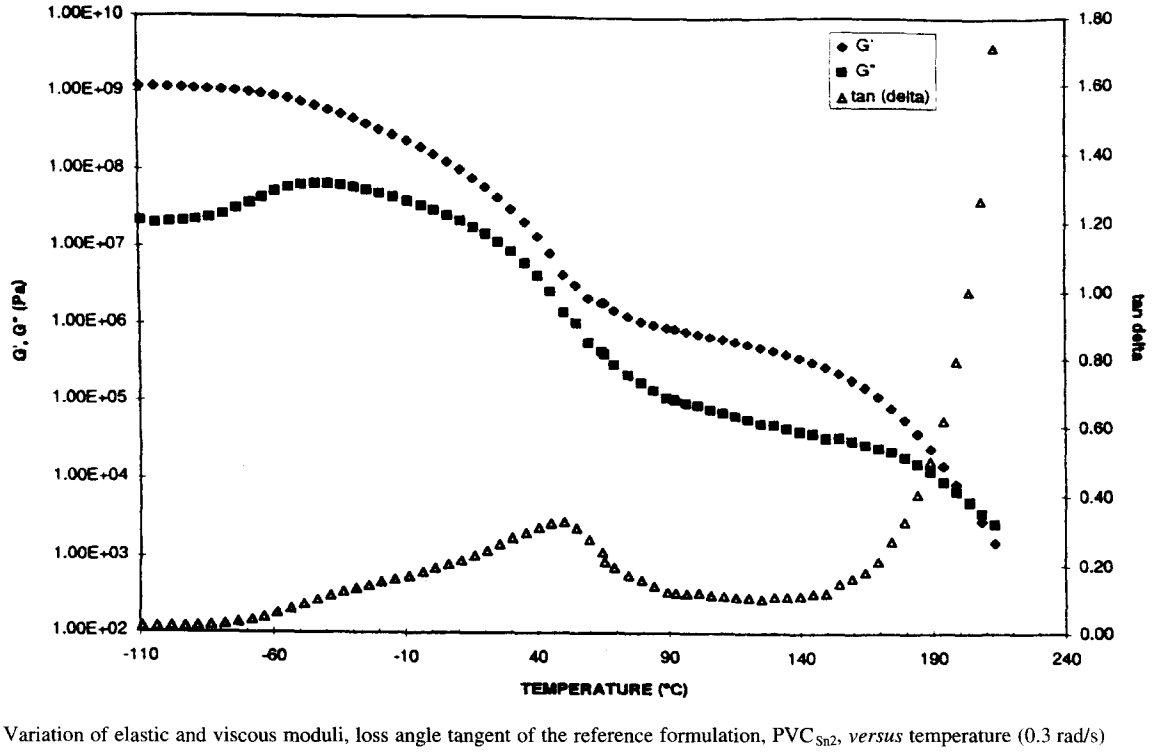

Figure 6 Variation of elastic and viscous moduli, loss angle tangent of the reference formulation, PVC_{Sn2}, *versus* temperature (0.3 rad/s)

An increase in draw ratio leads to a higher value of the modulus. This phenomenon has already been observed both for rigid and plasticized PVC, but in a lower temperature range [15,16]. The former studied the effect of drawing on plasticized PVC and noticed that the ultimate tensile strength increased up to a constant value with draw ratio (drawing at 40°C produced an increase in ultimate tensile strength of 67%, at 70°C the observed increase was 88% for a 20 phr DIOP-plasticized PVC). The latter observed that the Young's modulus reached a limiting value above a certain draw ratio. They explained this result as a diluting effect of plasticizer, in the presence of which drawing is less effective to orient polymer chains. In our case, drawing is carried out in the molten state and in the presence of the plasticizer. Robinson et al. [17] demonstrated through Raman and birefringence measurements that the presence of plasticizer allows the crystallites to be more highly oriented than the non-crystalline material, because it facilitates the rotation of the crystallites under drawing. So, the increase in Young's modulus observed in *Figure 8* may be accounted for by the orientation of crystallites under drawing; while for draw ratios higher than 15, the slight increase in Young's modulus may possibly be explained by a reduction in the effective cross-link density with increasing draw ratio, as suggested by Karacan et al. [18].

On the addition of talc in the previous formulation, the change of Young's modulus with draw ratio is shown in *Figure 9*: the shape of the curve is not modified and also

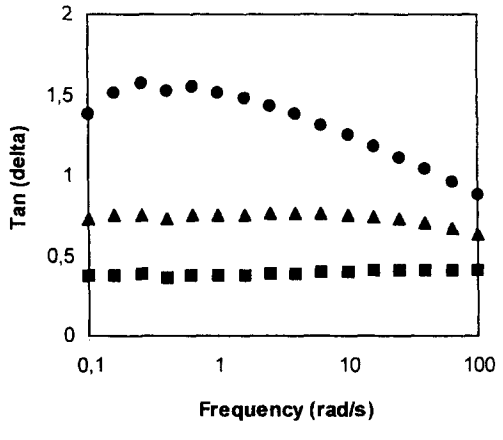

Figure 7 Variation of the loss angle tangent *versus* frequency and temperature for the reference formulation, PVC_{Sn2}. Different symbols are chosen according to temperature as follows: (●) 210°C, (▲) 200°C, (■) 190°C

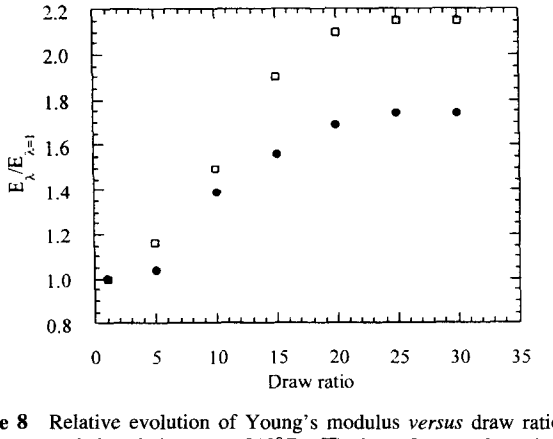

Figure 8 Relative evolution of Young's modulus *versus* draw ratio of samples extruded and drawn at 210°C: (□) the reference formulation, PVC_{Sn2} and (●) a 3 phr lead stabilizer-filled formulation, PVC_{Pb3}

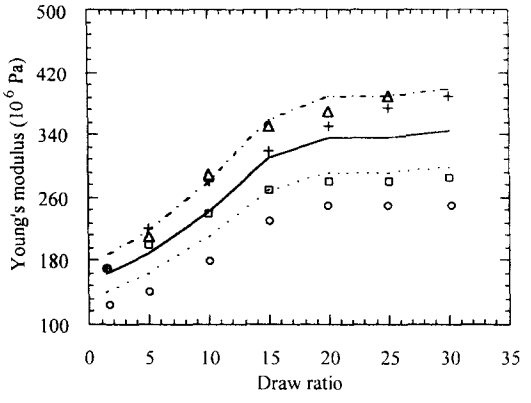

Figure 9 Variation of Young's modulus with draw ratio and talc concentration for samples extruded at 210°C. Symbols represent experimental data as follows: (□) PVC_{Sn2Ta4}; (+) PVC $_{Sn2Ta8}$; (△) PVC $_{Sn2Ta13}$; (○) PVC_{Sn2}, while dashed lines represent the theoretical model of Halpin and Tsai: (· · ·) PVC $_{Sn2Ta4}$; (-) PVC $_{Sn2Ta8}$; (- · -) PVC $_{Sn2Ta13}$

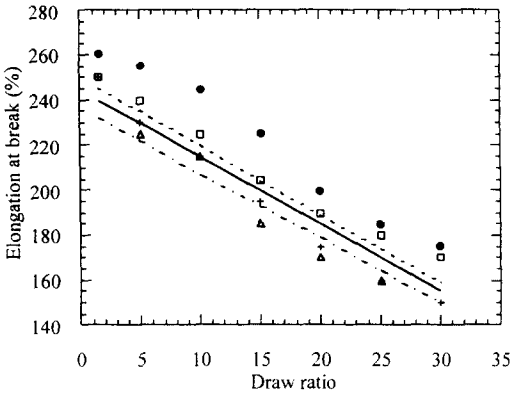

Figure 10 Variation of elongation at break with draw ratio and talc concentration for samples extruded at 210°C. Symbols represent experimental data as follows: (□) PVC_{Sn2Ta4}; (+) PVC $_{Sn2Ta8}$; (△) PVC $_{Sn2Ta13}$; (●) PVC_{Sn2}, while dashed lines represent the theoretical model of Nielsen:. (- - -) PVC $_{Sn2Ta4}$; (-) PVC $_{Sn2Ta8}$; (- · -) PVC $_{Sn2Ta13}$

presents a plateau at large draw ratios. Higher talc amounts increase tensile moduli. The enhancement of Young's modulus due to talc or other flake-like fillers has been reported in many cases [19–21] and correlated to an orientation of the platelet. For that reason, the predictive models for tensile modulus, e.g. the Halpin and Tsai law, take into account this phenomenon.

From the experimental data summarized in *Figure 9*, the ratio (E_c/E_m) is nearly constant whatever the draw ratio, while E_m depends on draw ratio, as shown previously in *Figure 8*. In order to compare our experimental results and the results obtained using the Halpin and Tsai law, we can propose the theoretical Young's modulus calculation as follows:

$$E_{\lambda c} = \frac{1 + \xi\eta\phi_p}{1 - \eta\phi_p} f(\lambda)(E_{\lambda m})_{\lambda=1} \qquad (12)$$

where $E_{\lambda c}$ is the modulus of the composite at draw ratio λ; $f(\lambda)$ is a function which depends only on λ at fixed processing conditions; $(E_{\lambda m})_{\lambda=1}$ is the initial modulus of the undrawn polymer matrix in the same processing conditions.

The dashed lines in *Figure 9* represent the results calculated according to equation (12) $[f(\lambda)(E_{\lambda m})_{\lambda=1}$ is taken as the experimental value of $E_{\lambda m}]$.

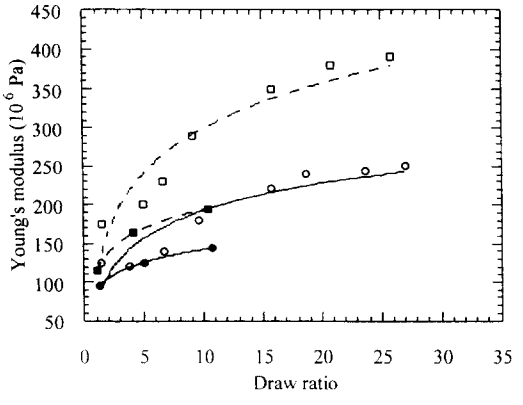

Figure 11 Comparison of Young's modulus versus draw ratio for samples extruded at 190 or 210°C. Symbols represent the experimental data, and lines the tendency of the curves: (●) $PVC_{Sn2/190°C}$; (○) $PVC_{Sn2/210°C}$; (■) $PVC_{Sn2Ta13/190°C}$; (□) $PVC_{Sn2Ta13/210°C}$

The Halpin–Tsai theory predicts the modulus behaviour of PVC talc-filled samples at each draw ratio well. This observation is in good agreement with X-ray diffraction measurements.

The elongation at break behaviour with talc concentration and draw ratio is given in *Figure 10*, where symbols represent experimental data.

An increase in talc concentration or draw ratio causes a decrease in elongation at break. The decrease observed with increasing draw ratio was expected since a drawn sample becomes less extensible. Higher amounts of talc are also expected to decrease the elongation at break, as suggested by the following equation (based on the Nielsen's law).

$$\epsilon_{\lambda c} = (1 - K\phi^{2/3})\epsilon_{(\lambda=1)m} g(\lambda) \qquad (13)$$

where $\epsilon_{\lambda c}$ is the composite elongation at break at draw ratio λ; $(\epsilon_{\lambda m})_{\lambda=1}$ is the elongation at break of the undrawn matrix at 210°C; $g(\lambda)$ is a function of draw ratio and is also correlated to the processing conditions.

K has been adjusted to a value of 1.4, and as shown in *Figure 10*, the experimental data fit the predictive model of Nielsen, developed for spherical particles with a good adhesion to the matrix. Generally, reinforcement is accompanied by a great loss of elongation at break, as demonstrated in the case of a PVC filled with mica in the study reported by Bataille et al. [22]. So, our results suggest that talc has a quite good adhesion to the matrix and does not induce a great loss in elongation at break.

Processing melt temperature $T = 190°C$

As previously said, it is interesting to also study the influence of the drawing temperature on tensile properties. The change of Young's modulus with draw ratio and draw temperature is shown in *Figure 11*. The maximum draw ratio (λ_{max}) which can be obtained depends greatly on draw temperature. Indeed, λ_{max} was about 35 at 210°C and 10 at 190°C. So, PVC can be more easily stretched in a liquid viscoelastic state. Stress–strain curves of rigid PVC in a temperature range from 95 to 180°C given by De Vries and Bonnebat [23] show that until PVC has a rubber-like behaviour, an increase in temperature leads to a smaller value of λ_{max}, and when it begins to flow (above 150°C), λ_{max} steadily increases to 7 (at 180°C). So, our results are in good agreement with these and, in the case of plasticized PVC, the maximum draw ratio which can be reached is higher.

Table 5 Variation of elongation at break with the extrusion temperature, formulations filled with talc

	$\lambda = 1.5$	$\lambda = 5$	$\lambda = 10$
PVC_{Sn2} 190°C	1.0	0.94	0.87
PVC_{Sn2} 210°C	1.0	0.98	0.92
$PVC_{Sn2Ta13}$ 190°C	1.0	0.90	0.72
$PVC_{Sn2Ta13}$ 210°C	1.0	0.92	0.84

For draw ratios up to 10, an increase in draw temperature tends to enhance Young's modulus. Some authors [17,18] have demonstrated that an increase in draw temperature promotes the orientation of the crystallites, while it permits a greater relaxation in the amorphous region. So, our results may be accounted for by assuming that crystallites are more oriented at 210°C, where PVC still has a viscoelastic gel state behaviour but also that of a viscoelastic liquid fluid. Addition of talc does not modify these conclusions (Young's modulus is moreover enhanced by the presence of the filler).

Table 5 gives the comparison of relative elongation at break behaviour.

An increase in extrusion temperature tends to enhance the elongation at break: for the same draw ratio, more extensibility still remains for a sample extruded at 210°C compared to 190°C (this observation is in agreement with the fact that the maximum draw ratio is higher at a more elevated extrusion temperature).

No difference between the X-ray diffractograms for samples extruded at the two temperatures was observed, leading us to think that the particle orientation is well achieved in the two cases.

Lead carboxylate particles

X-ray diffraction. A comparison of *Figures 12 and 13* shows that lead stabilizer is oriented after extrusion at 210°C. Low intensity peaks from *Figure 12* have disappeared, and we notice two types of reflecting planes (d = 8.654 and 3.313 Å) which are parallel to the extrudate surface, the other peaks correspond to high-order reflections of these two, as noted in *Figure 13*. In the absence of X-ray data concerning this compound, this systematic orientation of the particles cannot be documented. Higher diffraction intensities arise from the surface of the material. We attribute this difference to an enhancement of local stabilizer concentration near the extrudate surface insofar as we demonstrated previously [24] the external lubricant role of this lead stabilizer which migrates near the die walls.

So, as in the case of talc, the stabilizer particles are oriented parallel to the extrusion plane and this orientation is rather good from the smaller draw ratios. No difference in orientation distribution in the core and the skin was noticeable.

The stabilizer particles can also be aligned in the flow direction due to their ellipsoidal shape, as seen in *Figures 14 and 15*.

The pattern type and the reflection arcing, as in the case of fibres, illustrate a preferred orientation, here in the draw direction. Stabilizer orientation in the flow direction is limited in the presence of talc, as shown in *Figure 16*, which is typical of a more random-like distribution: the reflection arcing is less well defined.

Lim and White [7] have already noticed that the orientation of kevlar fibres dispersed in a polyethylene matrix is uniaxial in the presence of talc (or mica), whereas it is biaxial when used alone. In our case, the alignment of the

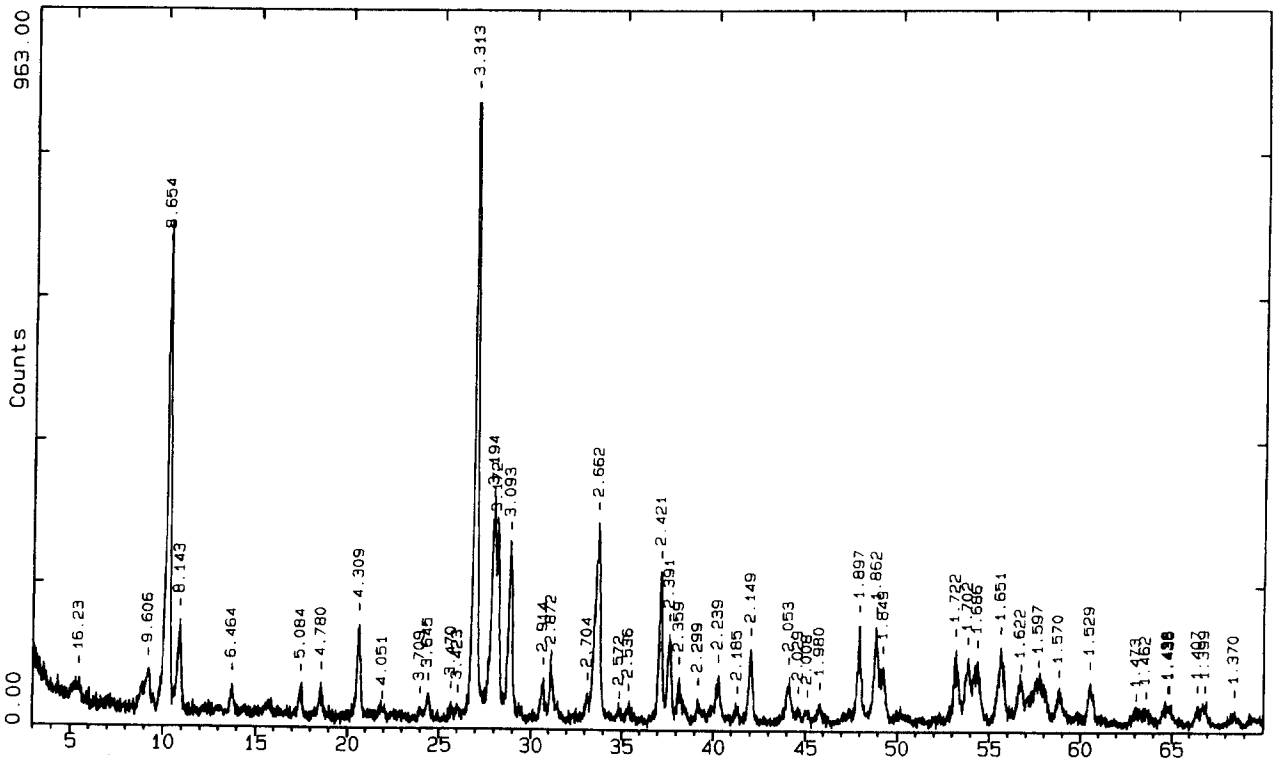

Figure 12 X-ray diffractometer scan of lead stabilizer alone (random orientation)

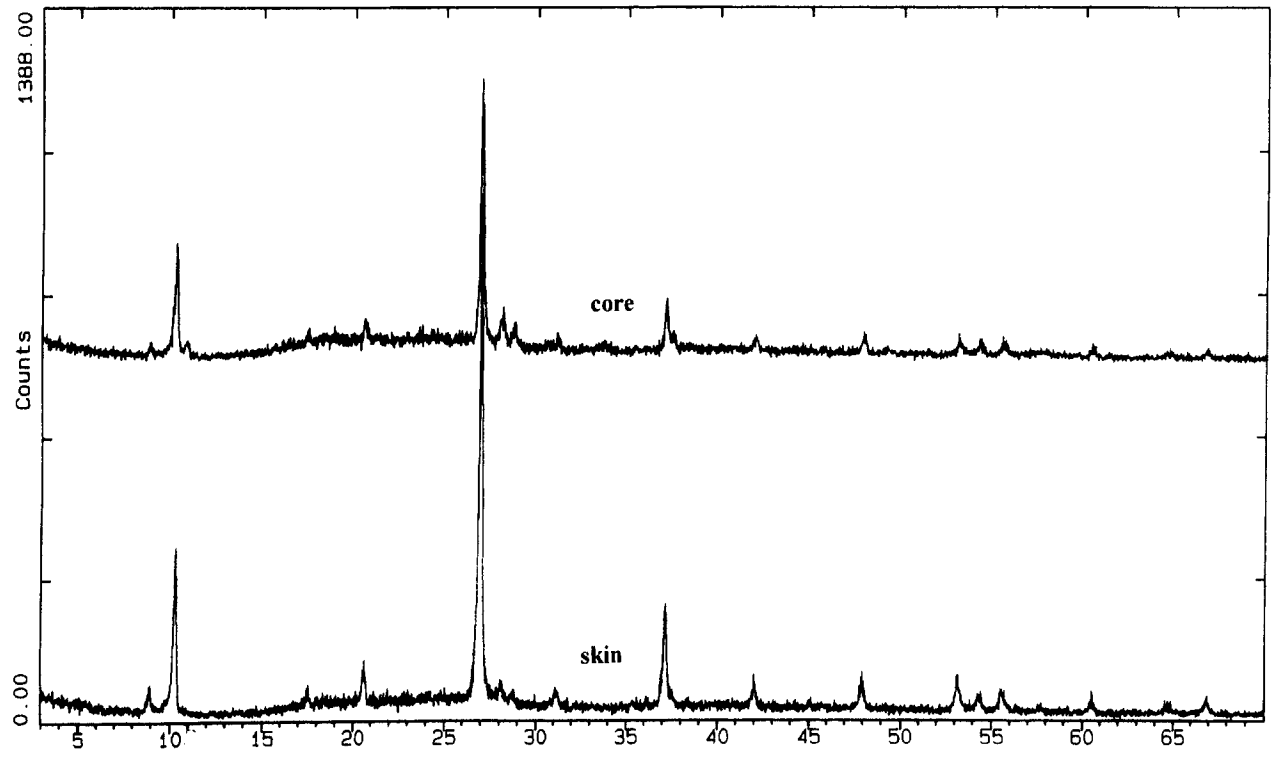

Figure 13 X-ray diffractometer scan of a 12 phr lead stabilizer-filled formulation drawn at 210°C with $\lambda = 2$, $PVC_{Pb12/\lambda=2/210°C}$

lead stabilizer particles along the draw direction seems to be hindered due to the presence of talc particles.

We also compared relative diffraction intensities for the sample $PVC_{Pb12/\lambda=5}$ extruded at 190 and 210°C in *Table 6*. The orientation of the lead stabilizer in the extrusion plane is represented by the peaks at $d = 3.33$ and 8.65 Å. Peaks arising elsewhere, e.g. at $d = 3.10$ and 3.17 Å, indicate that some lead carboxylate platelets are not well oriented. It clearly appears that the diffracted intensities from the $d = 3.33$ Å plane family are enhanced when the sample has been extruded at a higher temperature. This result suggests that when PVC tends to behave as a liquid viscoelastic fluid, the orientation of the lead stabilizer particles is promoted, maybe because of a greater flexibility of the chains.

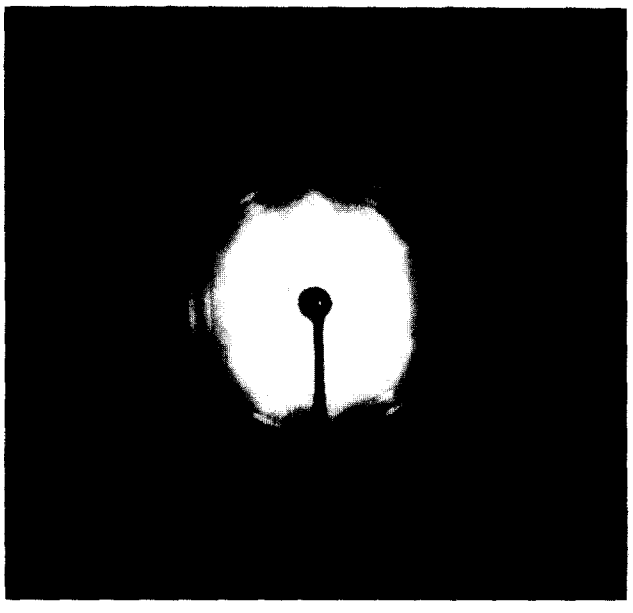

Figure 14 X-ray diffraction pattern (flat camera) of a 12 phr lead stabilizer-filled formulation drawn at 210°C with $\lambda = 26$, $PVC_{Pb12/210°C/\lambda=26}$

Figure 15 Transmission electron microscopy photo of a 12 phr lead stabilizer-filled formulation extruded at 210°C and cut parallel to the surface (× 6000; 1 cm: 166 μm)

Mechanical properties

Linear viscoelastic characterization

A temperature sweep in the glass transition region (the experimental procedure beeing the same as previously) leads to the curves representated in *Figure 17*. A shift of the α-transition towards higher temperatures is noticeable

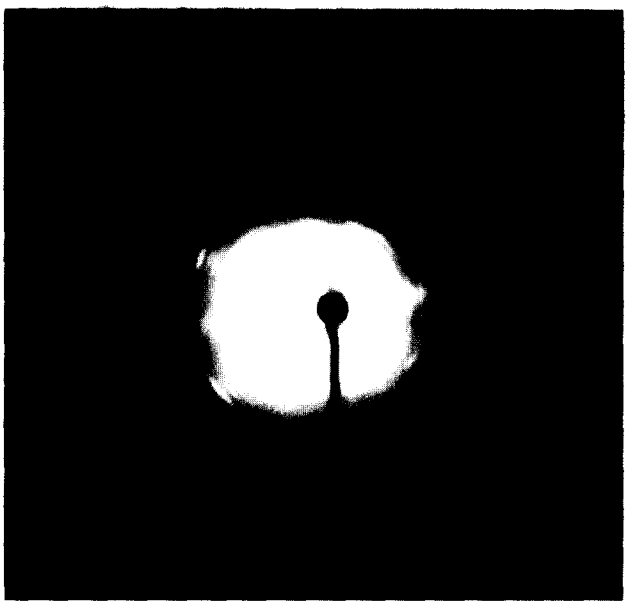

Figure 16 X-ray diffraction pattern (flat camera) of a 12 phr lead stabilizer and 13 phr talc-filled formulation extruded at 210°C and drawn with $\lambda = 29$, $PVC_{Pb12Ta13/210°C/\lambda=29}$

Table 6 Relative diffraction intensities of PVCPb12/$\lambda = 5$ extruded at 190 and 210°C

	$I_{d=3.33\ Å}/I_{d=8.62\ Å}$	$I_{d=3.33\ Å}/I_{d=3.17\ Å}$	$I_{d=3.33\ Å}/I_{d=3.10\ Å}$
PVC_{Pb12} 190°C, $\lambda = 5$	1.92	9.36	14.6
PVC_{Pb12} 210°C, $\lambda = 5$	3.25	13.4	16.7

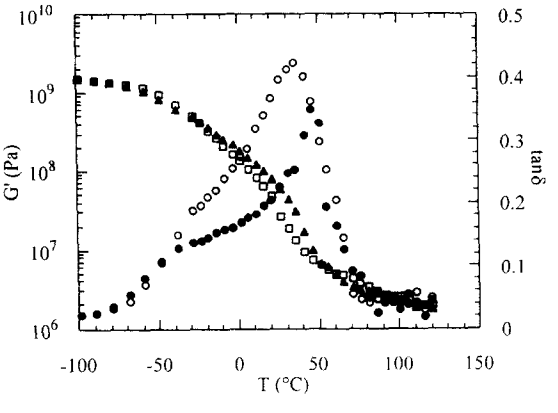

Figure 17 Variation of elastic modulus and loss angle tangent in the glass transition region when lead stabilizer is added at 4 or 12 phr. Elastic modulus G' is represented as follows: (●) PVC_{Pb4}; (□) PVC_{Pb12}, and tand is represented as follows: (○) PVC_{Pb4}; (●) PVC_{Pb12}

for the more concentrated lead stabilizer formulations, whereas the β-transition is unperturbed by this change in composition.

This result may be explained by the possible interactions developed between the lamellar lead stabilizer and the plasticizer, so that PVC becomes less 'plasticized' when increasing the lead stabilizer amounts.

The 'gel–liquid' transition temperature is not changed in the presence of the stabilizer, whatever the concentration, and is still equal to 205°C.

Processing melt temperature $T = 210$°C

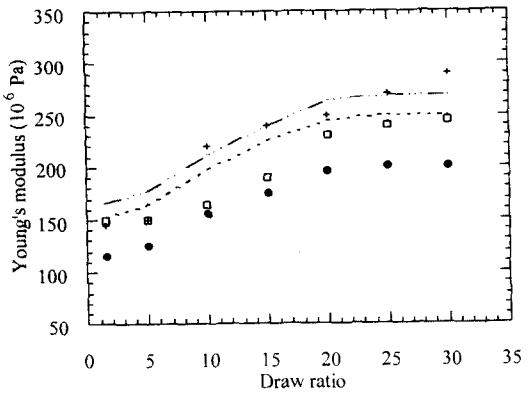

Figure 18 Variation of Young's modulus with draw ratio and lead stabilizer concentration for samples extruded and drawn at 210°C. Symbols represent experimental data as follows: (●) PVC_{Pb3}; (□) PVC_{Pb9}; (+) PVC_{Pb12}, dashed lines represent the theoretical model of Halpin and Tsai for (- - -) PVC_{Pb9} and (- · -) PVC_{Pb12}

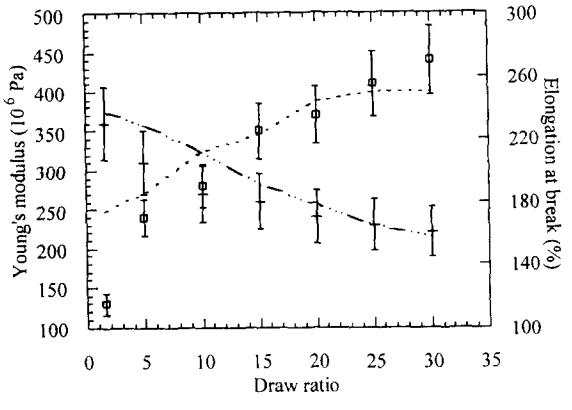

Figure 19 Variation of Young's modulus and elongation at break with draw ratio for a formulation extruded at 210°C and filled with 12 phr of lead stabilizer and 13 phr of talc, $PVC_{Pb12Ta13}$. Symbols represent experimental data: (□) Young's modulus and (+) elongation at break. Dashed lines represent the theoretical models: (- - -) Young's modulus and (- · -) elongation at break

The same analysis of the results as in the case of talc can be made. The formulation with the lowest lead stabilizer concentration is considered to be the unfilled matrix here, and its behaviour as a function of the draw ratio is reported in *Figure 18*. *Figure 18* gives the change of Young's modulus with stabilizer concentration and draw ratio, and compares experimental data with that related to the Halpin and Tsai law. If the lead stabilizer modulus is considered to be close to 5×10^9 Pa, the experimental data follow a similar trend to the predictive model of Halpin and Tsai.

The elongation at break also decreases with draw ratio, and its behaviour is well predicted by a modified Nielsen's law (with $K = 0.9$).

These tensile results coupled with that of X-ray diffraction lead us to the conclusion that lead stabilizer is well oriented under these extrusion conditions even at the lowest draw ratios. The enhancement produced by this lead carboxylate is lower than that due to talc because its own modulus is lower.

If the lead stabilizer and talc are added together in a formulation, we can determine the Young's modulus as follows:

$$E_{PVCPb12Ta13} = \frac{1 + \xi_t \eta_t \phi_t}{1 - \eta_t \phi_t} E_{PVCPb12} \tag{14}$$

where

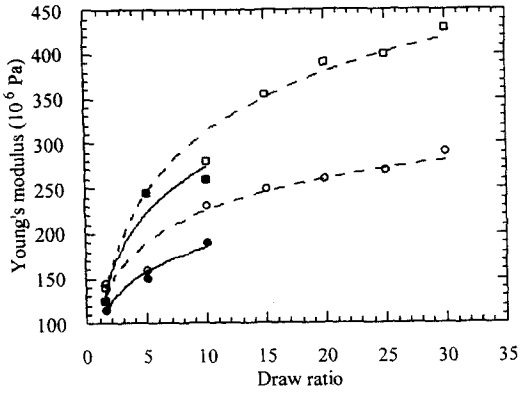

Figure 20 Variation of Young's modulus with draw ratio of samples extruded at 190 or 210°C, and filled with lead stabilizer and (or) talc. The lines represent the general tendency of the curves and the experimental data are represented by symbols as follows: (●) $PVC_{Pb12/190°C}$; (○) $PVC_{Pb12/210°C}$; (■) $PVC_{Pb12Ta13/190°C}$; (□) $PVC_{Pb12Ta13/210°C}$

$$\eta_t = \frac{E_t - E_{PVCPb12}}{E_t + \xi E_{PVCPb12}} \tag{15}$$

and E_t is the talc modulus.

$$E_{PVCPb12} = \frac{1 + \xi_s \eta_s \phi_s}{1 - \eta_s \phi_s} E_{PVCPb3} \tag{16}$$

$$\eta_s = \frac{E_s - E_{PVCPb3}}{E_s + \xi E_{PVCPb3}} \tag{17}$$

E_s is the lead stabilizer modulus.

So,

$$E_{PVCPb12Ta13} = \frac{1 + \xi_t \eta_t \phi_t}{1 - \eta_t \phi_t} \frac{1 + \xi_s \eta_s \phi_s}{1 - \eta_s \phi_s} E_{PVCPb3} \tag{18}$$

Elongation at break can also be written as:

$$\epsilon_{PVCPb12Ta13} = (1 - K_t \phi^{2/3})(1 - K_s \phi_s^{2/3}) \epsilon_{PVCPb3} \tag{19}$$

where $K_t = 1.4$ and $K_s = 0.9$; $\phi_t = 0.036$ and $\phi_s = 0.016$.

Tensile properties of the PVC filled with these two particle types are well predicted by equation (18)and equation (19), as shown in *Figure 19*.

Processing melt temperature $T = 190$°C

As seen before in the case of talc, an enhancement in Young's modulus is noticeable when the extrusion temperature is 210°C (*Figure 20*).

The main difference existing between these two temperatures is the larger draw ratio which can be obtained at 210°C. At 210°C, the polymer can be more stretched as it is in a liquid viscoelastic state.

CONCLUSION

X-ray diffraction measurements have enabled us to determine the orientation of talc and a lead stabilizer, considered here as a filler, in plasticized PVC extrudates. The lead carboxylate has proved to be better oriented when the draw temperature was 210°C, where PVC tends to behave as a liquid viscoelastic fluid. The presence of these two fillers enhances Young's modulus, with a good fitting of the Halpin and Tsai predictive model.

The extrudates were stretched below and above the 'gel–liquid' transition temperature. Above this temperature, the PVC can be far more stretched and the tensile results

suggest that the crystallites which are surrounded by more flexible chains are more oriented, in agreement with what is reported in the literature for a lower temperature range.

ACKNOWLEDGEMENTS

The authors wish to acknowledge the SYLEA firm for financial support of this study.

REFERENCES

1. Nielsen, L. E., *J. Compos. Mat.*, 1967, **1**, 100–119.
2. Manson, J. A. and Sperling, L. H., *Polymer Blends and Composites*, Plenum Press, New York, 1976.
3. Vincent, M. and Agassant, J. F., in *Two-phase Polymer Systems*, ed. L. A. Utracki, Chapter 11, Hanser Publishers, 1991.
4. Monge, G., Vincent, M. and Haudin, J. M., *Makromol. Chem., Macromol. Symp.*, 1987, **9**, 1–8.
5. Lim, S. H. and White, J. L., *J. Rheol.*, 1990, **34**(3), 343–366.
6. Crowson, R. J., Folkes, M. J. and Bright, P. F., *Polym. Engng Sci.*, 1980, **20**(14), 925–933.
7. Lim, S. H. and White, J. L., *Annu. Tech. Conf. Soc. Plast. Engng*, 1992, **50 (Vol.1)**, 1681–1684.
8. Darlington, M. W. and McGinley, P. L., *J. Mater. Sci.*, 1975, **10**(Letters), 906–910.
9. Sumita, M., Ookuma, T., Miyasaka, K. and Ishikawa, K., *Colloid Polymer Sci.*, 1984, **262**, 103–109.
10. Mitsuishi, K., Kodama, S. and Kawasaki, H., *J. Macromol. Sci. Phys.*, 1987, **B 26**(4), 479–494.
11. Halpin, J. C. and Kardos, J. L., *Polym. Engng Sci.*, 1976, **16**(5), 344–352.
12. Flores Flores, R., Comportement mécanique du PVC et de mélanges PVC/PMMA: effet de traitements thermiques et de la réticulation chimique. Thèse de doctorat, Université Lyon I, 1994.
13. Sahraoui, M., Etude des corrélations entre le comportement rhéologique du polychlorure de vinyle, sa microstructure et sa morphologie. Thèse de doctorat, Université Lyon I, 1990.
14. Aressy, M., Etude de l'influence de la nature des lubrifiants sur le phénomène de glissement du polychlorure de vinyle plastifié. Thèse de doctorat, Université Lyon I, 1994.
15. Liu, Z. and Gilbert, M., *Polymer*, 1987, **28**(July), 1303–1308.
16. King, J., Bower, D. I. and Maddams, W. F., *J. Appl. Polym. Sci.*, 1988, **35**, 787–796.
17. Robinson, M. E. R., Bower, D. I. and Maddams, B. P., *J. Polym. Sci.: Polym. Phys. Ed.*, 1978, **16**, 2115–2138.
18. Karacan, I., Bower, D. I. and Ward, I. M., *Polymer*, 1994, **35**(16), 3411–3422.
19. Vu-Khanh, T., Sanschagrin, B. and Fisa, B., *Polym. Compos.*, 1985, **6**(4), 249–260.
20. Arroyo Ramos, M., Sanchez-Berna, M. and Vigo Matheu, J. P., *J. Polym. Engng*, 1990, **9**(2), 85–104.
21. Zihlif, A. M. and Ragosta, G., *Mat. Lett.*, 1991, **11**(10,11,12), 368–372.
22. Bataille, P., Boisse, S. and Schreiber, H. P., *J. Vin. Techn.*, 1984, **6**(4), 147–151.
23. De Vries, A. J. and Bonnebat, C., *Polym. Engng Sci.*, 1976, **16**(2), 93–100.
24. Fras, I., Etude de l'influence de charges sur les phénomènes de glissement en filière et sur les propriétés mécaniques d'une gaine de câble électrique à base de poly(chlorure de vinyle) plastifié. Thèse de doctorat, Université Lyon I, 1996.